CT-Ultrasound Registration for Electromagnetic Navigation of Cardiac Intervention

Xingxin Liu[1], Lixu Gu[*]
School of Biomedical Engineering
Shanghai Jiao Tong University
Shanghai, China

Hongzhi Xie[2], Shuyang Zhang[2]
Department of Cardiothoracic Surgery
Peking Union Medical College Hospital
Beijing, China.

***Abstract*—The registration of ultrasound (US) and CT plays a vital role in clinical diagnosis and image-guided intervention. This research proposes a novel registration method combined with the electromagnetic navigation system for cardiac intervention. After a landmark-based method is carried out to get an initial registration, a 2D slice having the maximum similarity with the US image is generated from the 3D CT model. Finally, the SURF-based algorithm is used to register the 2D slice with the US image. The innovation lies in the integration of the intensity information and feature to register preoperative CT volume model with intra-operative US image in real time. Our method is validated by phantom and clinic experiments. The phantom experiment achieved an average FRE and TRE of 0.71±0.10mm and 0.96±0.17mm.**

Keywords: intra-operative 2D-3D registration; multi-modality registration; electromagnetic navigation;

I. INTRODUCTION

Thoracic aortic stent-grafts have been approved for the treatment of aneurysms in the thoracic descending aorta in recent years [1]. However, many patients cannot undergo the surgery due to advanced age, or severe comorbidities. Therefore, minimally invasive surgery based on surgical navigation is a better alternative to bring patients less pain and faster recovery without the need for sternotomy. The electromagnetic navigation system can track the surgical instruments in real-time and provide the surgeon with precise position and orientation of the instruments inside patient's body.

To improve the performance of surgical navigation, some researchers have focused on the work using intra-operative imaging such as computed tomography (CT), fluoroscopy, magnetic resonance imaging (MRI), and 3D ultrasound (US). However, these modalities have some disadvantages to limit their applications. In our research, 2D ultrasound is used to provide the intra-operative guidance in real time due to its security, low cost and ease to use. Image registration is vital to the surgical navigation. The fusion of the preoperative 3D CT image and the intra-operative 2D US image integrates the high quality and rich spatial information of the 3D CT with the real-time imaging ability of 2D US, providing the surgeon with complementary information acquired in the two different modalities and more precise guidance in the operation. Recently, most of the researches on CT/US registration are focus on the liver [2]. In this paper, we address that on the cardiac intervention. Considering the particular structures, we select the aortic valve, the outline of the atrium and ventricle etc. in the registration procedure.

There are two major groups of image registration methods for CT/US [3-5, 16-19]. One is the intensity-based method. Xu et al. [6] combined the mutual information (MI) and the normal vector information (NVI) into a single similarity measure to align the simulated US image from CT with the US image of the liver in radio frequency ablation. Wein et al. [7] registered US images to 3D CT by maximizing the cross-correlation. Another one is the feature-based method. Luo et al. [8] segmented the aortic root contour from short axis US image, then the points of contours were selected manually to register with the 3D CT aortic surface model. Terry et al. [9] extracted the feature points from aortic valve in the spatial registration after the temporal synchronization of the beating heart. However, they still have disadvantages respectively [10], the intensity-based method performs better for multi-modality image registration but is far more computationally intensive than the feature-based method, while the feature-based method has greater reliability but can be hard to distinguish between noise and edges. In this paper, we present a hybrid approach which encouraged by both merits from intensity and feature based methods to achieve more robust and accurate performance.

II. METHOD

A. GPU Accelerated Cardiac Modeling

In order to construct a 3D cardiac volume model for the preoperative planning and intra-operative navigation, patient's preoperative CT images are rendered by a raycasting algorithm [11], which implements the GPU acceleration with CUDA (Compute Unified Device Architecture) programming.

B. Preoperative Planning

According to the patient's condition, surgeons can determine the target position of the stent-graft and the path of surgical instruments on the cardiac volume model. The target position to deploy can be considered as a plane defined by a set of points distributed around the aneurysm.

C. Probe Calibration of US

In order to fuse the preoperative CT image with the intra-operative US image to assist the navigation, we apply a freehand method to calibrate the probe [12]. A 6-DOF sensor is attached to the probe and traced by the electromagnetic tracker. When scanning a customized phantom (Fig. 1) by the probe, a US image with high-intensity landmarks is acquired, then the point coordinate in the US image $P_{US}^{i}(1 \le i \le n)$ can be obtained, where n is the number of acquired keypoints. The point coordinate in the real world P_{world}^{i} determined by electromagnetic tracker are computed according to the coordinate of high-intensity landmarks in the US image and the coordinate of reference points in the real world. A point in US image transformed to the world coordinate can be represented by:

$$P_{world}^{i} = T_{world \leftarrow sensor} \cdot T_{sensor \leftarrow US} \cdot P_{US}^{i} \quad (1)$$

The $T_{world \leftarrow sensor}$ is the transform matrix from the tracking device coordinate to the world coordinate, and is measured by the electromagnetic tracker. The $T_{sensor \leftarrow US}$ is the calibration matrix from the US image coordinate to the tracking device coordinate, and is computed by:

$$T_{sensor \leftarrow US} = \underset{T}{\operatorname{argmin}} \sum_{i=1}^{n} \left\| T_{world \leftarrow sensor} \cdot T \cdot P_{US}^{i} - P_{world}^{i} \right\| \quad (2)$$

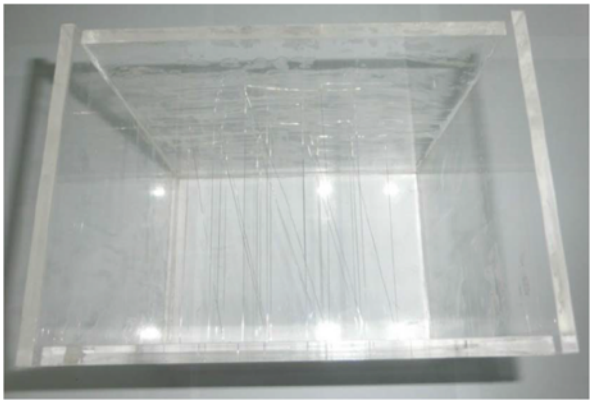

Figure 1. N-phantom for calibration

D. Registration

In order to register and fuse the intra-operative US image with the preoperative CT model, a spatial transform from any point in US image coordinate system P_{US}, to the corresponding point in 3D CT coordinate system P_{CT}, should be determined. The spatial transform $T_{CT \leftarrow US}$ is made up of three components as follows:

$$P_{CT} = T_{CT \leftarrow world} \cdot T_{world \leftarrow sensor} \cdot T_{sensor \leftarrow US} \cdot P_{US} \quad (3)$$

As the transform $T_{sensor \leftarrow US}$ is calculated in the calibration of US probe and fixed once the 6-DOF sensor is attached to the probe, and the $T_{world \leftarrow sensor}$ is measured in real time, the purpose of registration is to calculate and rectify the $T_{CT \leftarrow world}$, which is from the world coordinate to the preoperative CT coordinate.

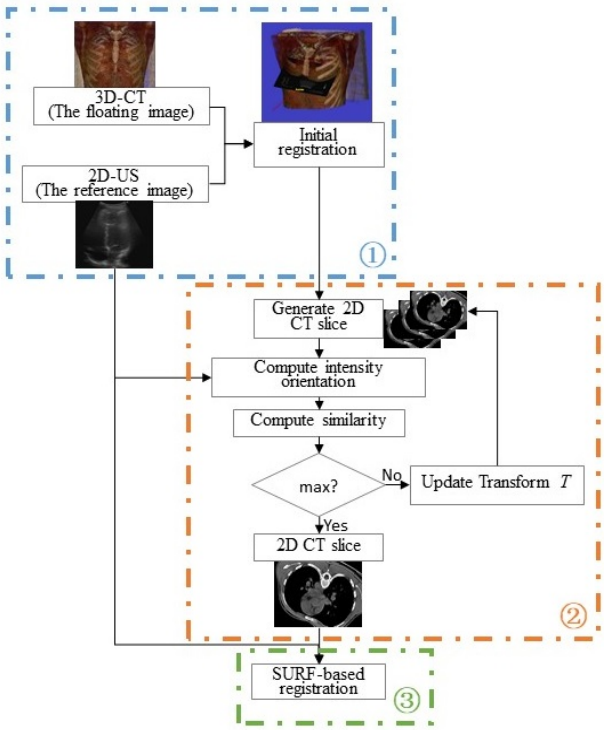

Figure 2. Workflow of our registration algorithm

According to the workflow in our system shown in Fig. 2, the registration in our research consists of two main steps, namely, initial registration and intra-operative registration. The initial registration is a rigid landmark-based transformation to get an initial transform matrix. In the intra-operative non-rigid registration, an intensity-based method is used to search for the CT slice having the maximum similarity with the US image, then a feature-based method is used to register this slice with the corresponding US image, and the transform is updated further.

1) Initial registration

We perform a landmark-based registration to gain an initial transform $T_{CT \leftarrow world}$. Several (6 in our research) fiducial landmarks within the target area on the phantom are selected. After reconstructing the preoperative 3D CT image of the phantom, these landmarks are identified in the image. Then a rigid transform is computed by minimizing the mean-squared distance between corresponding landmarks in the preoperative image and phantom.

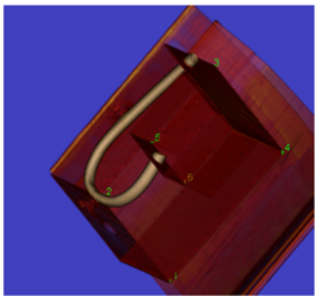

Figure 3. Fiducial landmarks selected for the initial registration

2) Intensity orientation-based registration

After initial registration, the intra-operative US image is registered and fused with the preoperative CT image approximately. Then a 2D slice of CT is extracted from 3D CT volume using the method of 3D cubic interpolation. The 2D slice has the same position, orientation and size with the US image.

The information of intensity orientation can be depicted by normal vector information (NVI) or gradient [13]. However, in 2D-2D registration based on NVI, some orientation information is ignored. Therefore, we propose a novel method to depict more complete intensity orientation information of a medical image. The intensity orientation of a pixel x in an image can be described by an eight-dimensional vector, each component of the vector represents the intensity difference between x and each of the eight-neighborhood pixels of x. The vector can be described as following:

$$\vec{v}(x)=\left[d_1,d_2,\ldots d_j\ldots,d_8\right]^T \tag{4}$$

where d_j is the intensity difference between x and its j-th neighboring pixel x_j. Considering that the intensity distribution in multi-modality medical images can be opposite, d_j is defined as:

$$d_j=\left(I(x)-I(x_j)\right)^2 \tag{5}$$

where $I(x)$ is the intensity of the pixel x, $I(x_j)$ is the intensity of its j-th neighboring pixel x_j. In order to eliminate the influence of outliers, the intensity orientation vector $\vec{v}(x)$ needs to be normalized.

For two images A and B, x_A in image A and x_B in image B are a pair of corresponding pixels. The similarity metric of x_A and x_B is defined as:

$$Metric(x_A,x_B)=\vec{v}(x_A)^T\,\vec{v}(x_B) \tag{6}$$

where the value of similarity metric is restrict to $[0,1]$. Ideally, if the two pixels share the same intensity orientation, the value of similarity metric will be 1. In our registration, the intra-operative US image is treated as the reference image R, and the 3D CT volume is treated as the floating image F. The goal is to search for the optimal transform T_{opt} to maximize the similarity of R, and the CT slice generated from the transformed floating image $T(F)$, as follows:

$$\begin{aligned}T_{opt}&=\arg\max_T Metric(R,F,T)\\&=\arg\max_T\frac{1}{N}\sum_{i=1}^{N}\vec{v}\left(R\left(x^{(i)}\right)\right)^T\vec{v}\left(T\left(F\left(x^{(i)}\right)\right)\right)\end{aligned} \tag{7}$$

where N is the number of the corresponding pixels $x^{(i)}$ in the common region of R and $T(F)$. A method of gradient descent is used to solve the optimization problem. The initial registration can provide an appropriate starting point to the optimization problem, so that the procedure converges more rapidly and avoids getting a local optimum. In each iteration, the transform T is updated and adopted to transform 3D CT volume, then a new 2D CT slice is generated for the next iteration. The updating is performed until the optimization algorithm converges, then the transform $T_{CT\leftarrow world}$ is rectified to be $T'(T_{opt}^{-1}\cdot T_{CT\leftarrow world})$.

3) Feature-based registration

While using the rectified transformation T' to transform the 3D CT volume, the 2D CT slice generated will have the maximum similarity with the US image. Nevertheless, due to the lack of spatial information in intensity orientation-based registration, a feature-based method should be used to register the 2D CT slice with the US image further.

In our research, the method of Speeded Up Robust Features (SURF) is adopted [14]. It's partly inspired by the scale-invariant feature transform (SIFT) descriptor, but it's several times faster than SIFT and is more robust in image registration. SURF uses a blob detector based on the Hessian matrix to find points of interest. The determinant of the Hessian matrix is used as a measure of local change around the point and points are chosen where this determinant is maximal. Given a point $\vec{p}=(x,y)$ in an image I, the Hessian matrix $H(\vec{p},\sigma)$ at point $\vec{p}$ and scale σ, is:

$$H(\vec{p},\sigma)=\begin{pmatrix}L_{xx}(\vec{p},\sigma) & L_{xy}(\vec{p},\sigma)\\ L_{xy}(\vec{p},\sigma) & L_{yy}(\vec{p},\sigma)\end{pmatrix} \tag{8}$$

where $L_{xx}(\vec{p},\sigma)$ is the convolution of the Gaussian second order derivative $\frac{\partial^2}{\partial x^2}I(\sigma)$ with the image I in point $\vec{p}$, and similarly for $L_{xy}(\vec{p},\sigma)$ and $L_{yy}(\vec{p},\sigma)$. To describe the descriptor around the point, a square region centered on the interest point is extracted. The interest region is split into smaller square sub-regions, and for each one, the Haar wavelet responses are extracted at sample points with regular space. In order to offer more robustness for deformations, noise and translation, the responses are weighted with a Gaussian. Then the descriptors are formed by summing up the wavelet responses over each sub-region.

Before the registration, the US image and the CT slice should be preprocessed to reduce noise. And regions of interest are extracted to reduce the computational complexity. Edges in the two images are detected using the canny detector. A suitable number of SURF points are defined by tuning the threshold of SURF detector. The threshold for the US image should be smaller to acquire more feature points due to its low imaging quality. By comparing the descriptors of points obtained from the two images, matching pairs are found. In order to eliminate the effect of outliers, we perform the method of random sample consensus (RANSAC) [15]. We scatter the whole matching pairs into some subsets randomly, calculate a transform on each subset, and merge these solutions into a weighted average as the final solution. Finally, the transform from the world coordinate

system to the CT image coordinate is rectified to be $T'' \cdot T'$, where T'' is the solution of the SURF-based registration.

III. RESULT

A. Data and Experimental Setup

The CT datasets of three healthy volunteers and two phantoms are acquired using a triphasic helical double-source computed tomography scanner (Cancer Hospital of Fudan University) with imaging parameters: slice thickness = 1.0mm, image resolution = 512 × 512, and spacing = 0.708984mm × 0.708984mm × 1mm. The US image with resolution = 720 × 576 is obtained from a GE LOGIQ P5 ultrasonic machine with a calibrated probe. The real-time US images are imported into our system with an image capture card. An electromagnetic tracking device (Aurora, Northern Digital Inc., Canada) is employed to track the pointer, the US probe and intervention instruments.

We developed the navigation system in Eclipse IDE using Python 2.7, and made full use of the classes from open-source visualization toolkits and libraries: VTK 6.3 (www.vtk.org), Atamai, CUDA 4.0 and OpenCV 2.4.9 (opencv.org).

B. Error

1) Fiducial Registration Error (FRE)

The FRE is defined as the root mean square of the difference between the fiducial landmarks selected on the 3D volume model and the corresponding positions on the phantom transformed by the $T_{CT \leftarrow world}$.

2) Target Registration Error (TRE)

The TRE is the total registration error including the calibration error of US probe, the offset of the pointer and so on. It's defined as the root mean square of the difference between the target positions determined in preoperative planning and the corresponding positions on the phantom transformed by the $T_{CT \leftarrow world}$.

C. Phantom Experiment

We customized a phantom (Fig. 4(a)) to present the cardiac structure, which was made by transparent plastic glass. The small cube in the phantom simulates the heart chamber, and the bend PVC pipeline simulates the descending aorta.

The preoperative CT image of the phantom was imported into our navigation system and reconstructed into a 3D model. Preoperative planning was performed on the model to determine the target position of stent-graft. The corners of the model were marked as the fiducial landmarks in the initial registration and compute the FRE. Some points on the aorta were selected as target points to compute TRE. After the initial registration and probe calibration were performed, the real-time US image was integrated into the system and fused with the 3D model approximately (Fig. 4(b)). When the tracked catheter was inserted into the bend pipeline, the system can visualize the model of stent-graft embedded in the front of the catheter and show the distance between the stent-graft and the target plane. Then the intensity orientation-based and SURF-based method were performed to fuse the model and US image better(Fig. 4(c)).

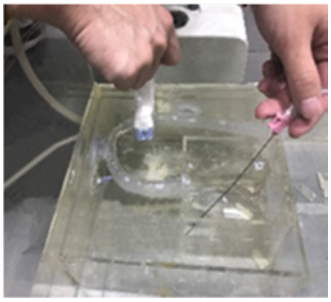

(a)

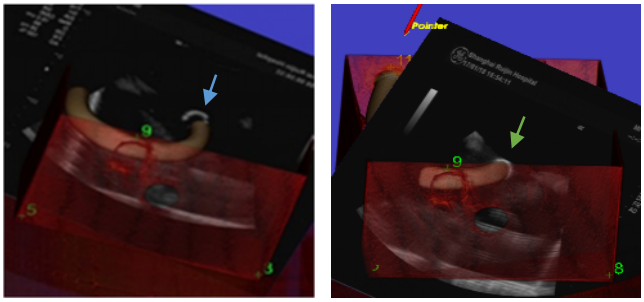

(b) (c)

Figure 4. The phantom experiment. (a) The experimental scene. (b) The fusion of the US image and 3D CT model after the initial registration. (c) The fusion images after the final registration.

The results of the phantom experiment are shown in Table I, demonstrating the accuracy and robustness of the registration. The average and standard deviation of root mean square of the residual distances of the fiducial and target points are listed. In order to validate the performance of the intensity orientation-based method, the final results are divided into two groups: the Final 1 without the step of intensity orientation-based registration, and the Final 2 within. The initial landmark-based registration achieves an average FRE and TRE of 0.75mm and 1.48mm. The TRE results are improved to an average of 0.96mm after using our hybrid method. In some cases, the FRE are increased slightly, due to the error introduced from the US probe calibration. In addition, the results of the Final 2 is better than those of the Final 1, which demonstrates that the intensity orientation-based method plays an important role in the whole registration. By contrasting with the results of other methods, our method is more accurate and robust.

TABLE I. FRE (MM) AND TRE (MM) OF REGISTRATION. (FINAL 1 IS THE RESULT WITHOUT THE INTENSITY ORIENTATION-BASED REGISTRATION, WHILE FINAL 2 WITHIN)

	Initial		**Final 1**		**Final 2**	
	FRE	***TRE***	***FRE***	***TRE***	***FRE***	***TRE***
1	0.82	1.45	0.77	1.12	0.68	0.91
2	0.77	1.42	0.75	1.05	0.70	0.87
3	0.69	1.64	1.19	1.35	0.91	1.29
4	0.83	1.50	0.80	1.03	0.65	0.88
5	0.65	1.39	0.75	0.98	0.62	0.85
	0.75 ±0.07	1.48 ±0.09	0.85 ±0.17	1.11 ±0.13	0.71 ±0.10	0.96 ±0.17

D. Clinical Experiment

The CT datasets of three healthy volunteers were obtained to further evaluate the performance of our system. The short axis US images of apical four-cavity were chosen to register, where the structure of the atrium, ventricle, and mitral valve is clearly visible.

Fig. 5(a) shows the fusion of the 3D volume model and the US image after running our registration algorithm. In order to show more details, the US image and the corresponding 2D slice from the 3D volume model are shown in Fig. 5(b). It can be seen that the corresponding structures and features of the two images are well aligned.

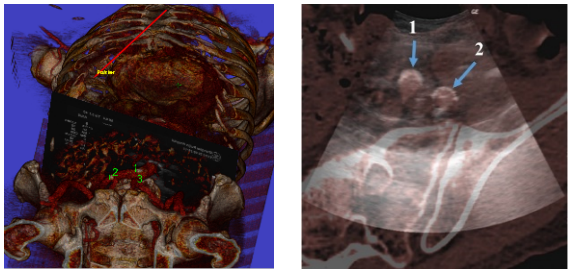

(a) (b)

Figure 5. The clinical experiment. (a) The fusion images. (b) The details of the fusion (1 and 2: two vessels).

IV. CONCLUSION

In this paper, we proposed a novel registration method combining the intensity information and feature of images. To our knowledge, the traditional approaches of multi-modality registration usually need extensive manual effort to extract feature points or contours. Those manual steps can be avoided using our algorithm. On the other hand, our method achieves a trade-off between the accuracy, robustness and computation complexity. The method of SURF is more robust against different image transformations than SIFT, and its combination with the intensity-based method can improve the accuracy of registration. In addition, the initial registration provides an appropriate starting point to the optimization problem of the intra-operative registration, so that the computation complexity can be reduced significantly. Experiments demonstrated that our method is acceptable in medical diagnosis and thoracic aortic stent-graft deployment.

ACKNOWLEDGMENT

This research is partially supported by the National Key research and development program (2016YFC0106200), and 863 national research fund (2015AA043203) as well as the Chinese NSFC research fund (61190120, 61190124 and 61271318).

REFERENCES

[1] M. Dake, D. Miller, C. Semba, R. Mitchell, P. Walker and R. Liddell, "Transluminal Placement of Endovascular Stent-Grafts for the Treatment of Descending Thoracic Aortic Aneurysms", New England Journal of Medicine, vol. 331, no. 26, pp. 1729-1734, 1994.

[2] L. Crocetti, R. Lencioni, S. DeBeni, T. See, C. Pina and C. Bartolozzi, "Targeting Liver Lesions for Radiofrequency Ablation", Investigative Radiology, vol. 43, no. 1, pp. 33-39, 2008.

[3] Derek L G Hill, Philipp G Batchelor, Mark Holden and David J Hawkes, “Medical image registration”, Physics in Medicine and Biology, Volume 46, Number 3, 2001

[4] T. Makela ; P. Clarysse ; O. Sipila ; N. Pauna ; Quoc Cuong Pham ; T. Katila ; I.E. Magnin, “A review of cardiac image registration methods”, IEEE Transactions on Medical Imaging, Volume 21, Issue 9, Sept. 2002

[5] P. Markelj, P. MarkeljEmail the author P. Markelj, D. Tomaževič, B. Likar, F. Pernuš, “A review of 3D/2D registration methods for image-guided interventions”, Medical Image Analysis, Volume 16, Issue 3, Pages 642–661, April 2012

[6] L. Xu, J. Liu, W. Zhan and L. Gu, "A novel algorithm for CT-ultrasound registration", 2013 IEEE Point-of-Care Healthcare Technologies, 2013.

[7] W. Wein, S. Brunke, A. Khamene, M. Callstrom and N. Navab, "Automatic CT-ultrasound registration for diagnostic imaging and image-guided intervention", Medical Image Analysis, vol. 12, no. 5, 2008.

[8] Z. Luo, Q. Zhao, J. Cai, S. Wang and L. Gu, "Electromagnetic Navigation for Thoracic Aortic Stent-graft Deployment Using Tracked Ultrasound", IFMBE Proceedings, pp. 2130-2133, 2013.

[9] Xishi Huang, J. Moore, G. Guiraudon, D. Jones, D. Bainbridge, Jing Ren and T. Peters, "Dynamic 2D Ultrasound and 3D CT Image Registration of the Beating Heart", IEEE Transactions on Medical Imaging, vol. 28, no. 8, pp. 1179-1189, 2009.

[10] R. McLaughlin, J. Hipwell, D. Hawkes, J. Noble, J. Byrne and T. Cox, "A Comparison of 2D-3D Intensity-Based Registration and Feature-Based Registration for Neurointerventions", Medical Image Computing and Computer-Assisted Intervention — MICCAI 2002, pp. 517-524, 2002.

[11] Scharsach H. “Advanced GPU Raycasting”. In: Central European Seminar on Computer Graphics,2005: 69-76.

[12] F. Lindseth, G. Tangen, T. Langø and J. Bang, "Probe calibration for freehand 3-D ultrasound", Ultrasound in Medicine & Biology, vol. 29, no. 11, pp. 1607-1623, 2003.

[13] E. Haber and J. Modersitzki, "Intensity Gradient Based Registration and Fusion of Multi-modal Images", Methods of Information in Medicine, 2007.

[14] H. Bay, T. Tuytelaars and L. Van Gool, "SURF: Speeded Up Robust Features", Computer Vision – ECCV 2006, pp. 404-417, 2006.

[15] M.A. Fischler and R.C. Bolles. “Random sample consensus: A paradigm for model fitting with applications to image analysis and automated cartography”. Communications of the ACM, 24(6):381–395, 1981

[16] Thomas Lange, Nils Papenberg, Stefan Heldmann, Jan Modersitzki, Bernd Fischer, Hans Lamecker, Peter M. Schlag. “3D ultrasound-CT registration of the liver using combined landmark-intensity information”. International Journal of Computer Assisted Radiology and Surgery. Volume 4, Issue 1, pp 79–88, January 2009

[17] Susanne Winter, Bernhard Brendel, Ioannis Pechlivanis, Kirsten Schmieder and Christian Igel. “Registration of CT and Intraoperative 3-D Ultrasound Images of the Spine Using Evolutionary and Gradient-Based Methods”. IEEE Transactions on Evolutionary Computation, Volume: 12, Issue: 3, pp. 284-296, June 2008

[18] W. H. Nam, D. G. Kang, D. Lee, J. Y. Lee and J. B. Ra. “Automatic registration between 3D intra-operative ultrasound and pre-operative CT images of the liver based on robust edge matching”. Physics in Medicine & Biology, Volume 57, Number 1, 29 November 2011

[19] J.H. Kaspersen, E. Sjolie, J. Wesche, J. Asland, J. Lundbom, A. Odegard, F. Lindseth and T.A. Nagelhus Hernes. “Three-Dimensional Ultrasound-Based Navigation Combined with Preoperative CT During Abdominal Interventions: A Feasibility Study”. CardioVascular and Interventional Radiology, Volume 26, Issue 4, pp. 347–356, August 2003